Impact of 2D–3D Heterointerface on Remote Epitaxial Interaction through Graphene

Impact of 2D-3D Heterointerface on Remote Epitaxial Interaction through Graphene

Journal:	*ACS Nano*
Manuscript ID	nn-2021-03296s.R3
Manuscript Type:	Article
Date Submitted by the Author:	n/a
Complete List of Authors:	Kim, Hyunseok; Massachusetts Institute of Technology, Lu, Kuangye; Massachusetts Institute of Technology Liu, Yunpeng; Massachusetts Institute of Technology Kum, Hyun; Massachusetts Institute of Technology, Mechanical Engineering Kim, Ki Seok; Massachusetts Institute of Technology Qiao, Kuan; Massachusetts Institute of Technology Bae, Sang-Hoon; Massachusetts Institute of Technology Lee, Sangho; Massachusetts Institute of Technology, Department of Materials Science and Engineering Ji, You Jin; Sungkyunkwan University College of Engineering Kim, Ki Hyun; Sungkyunkwan University - Suwon Campus, Advanced Materials Science and Engineering Paik, Hanjong; Cornell University, Department of Materials Science and Engineering Xie, Saien; Cornell University, Shin, Heechang; Yonsei University Choi, Chanyeol; Massachusetts Institute of Technology, Mechanical Engineering Lee, June Hyuk; Korea Atomic Energy Research Institute Dong, Chengye; The Pennsylvania State University Robinson, Joshua A.; Pennsylvania State University, Materials Science & Engineering Lee, Jae-Hyun; Ajou University, Materials Science and Engineering Ahn, Jong-Hyun; Yonsei University, School of Electrical and Electronic Engineering Yeom, Geun Young; Sungkyunkwan University, Advanced Materials Science and Engineering Schlom, Darrell; Cornell University, Dept. of Materials Science & Engineering Kim, Jeehwan; Massachusetts Institute of Technology,

Impact of 2D-3D Heterointerface on Remote Epitaxial Interaction through Graphene

*Hyunseok Kim,[1,†] Kuangye Lu,[1,†] Yunpeng Liu,[1] Hyun S. Kum,[1] Ki Seok Kim,[2] Kuan Qiao,[1] Sang-Hoon Bae,[1] Sangho Lee,[1,3] You Jin Ji,[4] Ki Hyun Kim,[4] Hanjong Paik,[5] Saien Xie,[5,6] Heechang Shin,[7] Chanyeol Choi,[8] June Hyuk Lee,[9] Chengye Dong,[10,11] Joshua A. Robinson,[10,11] Jae-Hyun Lee,[12] Jong-Hyun Ahn,[7] Geun Young Yeom,[4,13] Darrell G. Schlom[5,6,14] and Jeehwan Kim[1,2,3,15]**

AUTHOR ADDRESS

[1]Department of Mechanical Engineering, Massachusetts Institute of Technology, Cambridge, MA 02139, USA

[2]Research Laboratory of Electronics, Massachusetts Institute of Technology, Cambridge, MA 02139, USA

[3]Department of Materials Science and Engineering, Massachusetts Institute of Technology, Cambridge, MA 02139, USA

[4]School of Advanced Materials Science and Engineering, Sungkyunkwan University, Suwon 16419, Republic of Korea

[5]Department of Materials Science and Engineering, Cornell University, Ithaca, NY 14850, USA

[6]Kavli Institute at Cornell for Nanoscale Science, Ithaca, NY 14850, USA

[7]School of Electrical and Electronic Engineering, Yonsei University, Seoul 03722, Republic of Korea

[8]Department of Electrical Engineering and Computer Science, Massachusetts Institute of Technology, Cambridge, MA 02139, USA

[9]Neutron Science Division, Korea Atomic Energy Research Institute, Daejeon 34057, Republic of Korea

[10]Department of Materials Science and Engineering, The Pennsylvania State University, University Park, Pennsylvania 16802, USA

[11]2D Crystal Consortium, The Pennsylvania State University, University Park, Pennsylvania 16802, USA

[12]Department of Energy Systems Research and Department of Materials Science and Engineering, Ajou University, Suwon 16499, Republic of Korea

[13]SKKU Advanced Institute of Nano Technology (SAINT), Sungkyunkwan University, Suwon 16419, Republic of Korea

[14]Leibniz-Institut für Kristallzüchtung, Berlin 12489, Germany

[15]Microsystems Technology Laboratories, Massachusetts Institute of Technology, Cambridge, MA 02139, USA

† These authors contributed equally.

ABSTRACT

Remote epitaxy has drawn attention as it offers epitaxy of functional materials that can be released from the substrates with atomic precision, thus enabling production and heterointegration of flexible, transferrable, and stackable freestanding single-crystalline membranes. In addition, the remote interaction of atoms and adatoms through two-dimensional (2D) materials in remote epitaxy allows investigating and utilizing electrical/chemical/physical coupling of bulk (3D) materials *via* 2D materials (3D-2D-3D coupling). Here, we unveil the respective roles and impacts of the substrate material, graphene, substrate-graphene interface, and epitaxial material for electrostatic coupling of these materials, which governs cohesive ordering and can lead to single-crystal epitaxy in the overlying film. We show that simply coating a graphene layer on wafers does not guarantee successful implementation of remote epitaxy, since atomically precise control of the graphene-coated interface is required, and provide key considerations for maximizing the remote electrostatic interaction between the substrate and adatoms. This was enabled by exploring various material systems and processing conditions, and we demonstrate that the rules of remote epitaxy vary significantly depending on the ionicity of material systems as well as the graphene-substrate interface and the epitaxy environment. The general rule of thumb discovered here enables expanding 3D material libraries that can be stacked in freestanding form.

KEYWORDS

remote epitaxy; graphene; single-crystal membrane; transfer process; ionicity; heterointegration;

Freestanding semiconductor thin films are game-changing building blocks for flexible, conformal, and heterostructured electronic/photonic devices. In conventional approaches to attain freestanding membranes, single-crystalline semiconductor layers are first epitaxially grown on semiconductor wafers, followed by detaching the grown layer from the wafers. The key challenge in these approaches is separating the epitaxial layer from the substrate, because the layer and the substrate are connected through strong bonds.[1] There have been several techniques proposed to tackle this challenge, such as employing a sacrificial layer,[2] melting the interface by lasers,[3] mechanically spalling the film,[4] or completely etching away the wafer[5]; however, these methods have limitations in terms of applicable choice of materials, throughput, cost, or interface quality.[1] Recently, remote epitaxy has been proposed as an approach that can overcome these limitations and realize high-quality single-crystalline membranes.[6] In remote epitaxy, epitaxy is conducted on the wafer coated with graphene, wherein electrostatic potential of the substrate is not completely screened by graphene, which allows remote interaction between the substrate and the epilayer and enables the epilayer to follow the crystalline template of the substrate. Due to the weak van der Waals bonding between the graphene and the epilayer, the grown layer can be peeled off precisely at the graphene interface, thereby providing a simple and ideal pathway to form freestanding single-crystalline membranes. Remote epitaxy and graphene-mediated exfoliation have been demonstrated for several material systems, including III-V, III-N, II-VI, perovskites, and other complex oxides,[6-13] showing the versatility of the approach for diverse applications and heterogeneous integration.

Although the underlying physics and principles of remote epitaxy are theoretically investigated,[7,9,14,15] experimental environments could be vastly different from the general assumptions used in theoretical study, which is that both the substrate and the graphene layer are

pristine without any defects, residue, or contamination. Furthermore, even if graphene-coated substrates are prepared satisfying such conditions, the harsh epitaxy environment could also alter the graphene or the substrate properties and thus influence the formation of remote epitaxial films. Therefore, considering such factors are imperative for tailoring the remote interaction between adatoms and substrates for cohesive ordering of remote epitaxial layers, and furthermore, could bring insights in unveiling the respective roles and impacts of the substrate, graphene, their interface, and epitaxial material for coupling of these materials. Only with rigorous characterizations in each experimental step combined with theory, can these phenomena be unambiguously studied without confusion. Here, we show how the graphene and the interface properties can affect the electrostatic coupling of functional semiconducting and complex-oxide materials, wherein the coupling strength governs the nucleation of adatoms and thus affects the properties of remote epitaxial films. We demonstrate that the interface between the graphene and the substrate plays a critical role in remote epitaxy. Characterization of graphene and the substrate reveal that the quality of the interface varies depending on the graphene transfer methods, thereby affecting remote epitaxial interaction through graphene. Such effects are investigated in III-V, III-N, and complex oxide materials, which have different ionicity and thus different degree of remote interaction strength. We also demonstrate that graphene properties can be changed during epitaxy and such alteration can lead to failure of remote epitaxial growth, depending on the epitaxy conditions employed. Lastly, the nature of remote interaction through graphene is investigated by involving non-polar materials in graphene-mediated epitaxy, from which other possibilities of epitaxy modes besides remote epitaxy could be ruled out. These results provide critical aspects for experimental studies of remote epitaxy on various material systems, and brings insights in understanding 3D-2D-3D coupled material systems.

Results and discussion

It is well understood that electrical, mechanical, and chemical properties of graphene can be greatly altered if graphene is transferred from the host substrate to another foreign substrate. This is because graphene can be wrinkled, torn, contaminated with residue, or chemically doped depending on the transfer method,[16] and in this regard, remote interaction of adatoms on graphene-coated substrates can also be severely affected by graphene transfer methods. Here, we employ two widely used and representative techniques—a wet transfer method and a dry transfer method—to study the impact of interface properties on transmission of epitaxial fields. First, monolayer graphene was wet-transferred on growth substrates, wherein polymer/graphene stacks were scooped with wafers in deioinized water[17] (see Methods for a detailed process). Then, monolayer graphene was dry-transferred by utilizing metal-induced layer resolved transfer, where the graphene was peeled from a SiC substrate and immediately dry-transferred on the growth substrate[18,19](see Methods). GaAs, GaN, $SrTiO_3$ (STO), and Ge substrates are used as growth substrates to investigate the effect of ionicity of substrate materials on remote epitaxy, each representing III-V, III-N, complex oxides, and group IV families. The quality of chemical vapor deposition (CVD)-graphene and epitaxial graphene is confirmed by transferring the graphene onto a SiO_2/Si substrate by wet and dry transfer, respectively. The Raman spectra of these samples show the 2D peak position of ~2680 cm^{-1} and low *I(D)/I(G)* ratio of < 0.1, revealing that both graphene layers have monolayer thickness with low defect density[20,21] (Supporting Figure S1). The quality of graphene is maintained after transferring it onto semiconductor wafers, and the graphene-coated GaAs surfaces exhibit the surface roughness below 1 nm for both transfer methods (See Supporting Figure S1 and S2). The quality of graphene is also corroborated through X-ray photoelectron spectroscopy (XPS) characterization on graphene-coated GaAs wafers (Figure 1a and 1c) as it

shows dominant sp^2 bonding with small portion of sp^3 bonding-related peaks for both wet- and dry-transferred graphene.[22] The full-width at half-maximum (FWHM) linewidths of sp^2 component of wet- and dry-transferred graphene are in the range of 1.3 ± 0.2 eV (Figure 1a, 1c and Supporting Figure S3), confirming that transferred graphene exhibits high material quality with minimal broadening of sp^2 peaks.[23]

While graphene maintains its original quality after transferring onto the wafers regardless of transfer methods, we discovered that the properties of graphene-substrate interfaces can be varied by the graphene transfer history. In order to ensure propagation of the electrostatic potential from the substrate through graphene into epitaxial films, the distance between the epitaxial films and the substrate must be minimized, meaning that any contaminant or oxide formation at the graphene/substrate interface can easily disturb the propagation of the electrostatic potential resulting in a lack of remote epitaxy. Thus, we have attempted to strip the native oxides on the substrate right before transferring graphene on the wafer. During wet transfer process, for example, we have deoxidized GaAs substrates right before scooping the poly(methyl-methacrylate) (PMMA)/graphene layer from water. For dry transfer, we peeled graphene from SiC substrates and removed native oxides on GaAs right before transferring graphene to GaAs substrates in our effort to produce a pristine interface. Despite these efforts, however, our XPS analysis on graphene-coated GaAs substrates revealed that wet-transferred graphene on GaAs exhibits strong peaks related to native oxides, such as As_2O_3 and Ga_2O_3 (Figure 1b and Supporting Figure S4).[22] These results imply that wet transfer may not offer pristine graphene-substrate interfaces as trapped water at the interface contribute to substrate oxidation during drying process. On the other hand, our XPS analysis found out that these native oxide peaks are negligible in dry-transferred graphene, which confirms that dry-transferred graphene makes pristine contact on a hydrophobic GaAs wafer

after stripping the oxide. After sealing the GaAs surface with graphene, further oxidation no longer occurs since oxygen cannot penetrate through graphene.[24,25]

Next, we grew epitaxial GaAs on GaAs (100) substrates covered with wet- and dry-transferred graphene by metal-organic chemical vapor deposition (MOCVD) using nitrogen as the carrier gas (See detailed growth conditions in Methods). As shown in Figure 1e, the GaAs layer grown on wet-transferred graphene did not fully coalesce, and randomly oriented facets are observed. On the other hand, GaAs grown on dry-transferred graphene shows a fully coalesced film (see Figure 1f). Both samples are successfully exfoliated by depositing a nickel stressor and attaching thermal release tape (See detailed exfoliation process in Methods). Electron backscatter diffraction (EBSD) maps measured from the exfoliated film at the interface side reveal that the GaAs film grown on wet-transferred graphene is polycrystalline, unlike GaAs on dry-transferred graphene which is (100)-oriented single crystal, as shown in Figure 1e and 1f. These results can be directly correlated to the XPS spectra representing the oxidation of GaAs surface when wet transfer method is employed. It is also consistent with the previous report that the ionicity of materials is the key factor enabling remote epitaxy. The ionicity of GaAs is relatively small, allowing only monolayer-thickness graphene to provide enough substrate electrostatic potential penetration for remote interaction with adatoms.[7] Since surface oxides of GaAs further widens the gap between the substrate GaAs crystal and the graphene, the penetration of electrostatic potential fluctuation through graphene is not strong enough to remotely seed the GaAs overlayer when the GaAs surface is oxidized. Thus, it clearly shows the impact of interface properties on the strength of adatom-substrate remote interaction, and suggests that the dry-transfer must be carried out to prevent the III-V substrate from oxidation for remote epitaxy. Because epitaxial graphene on SiC, which is employed here for dry transfer, is not readily available due to the high cost of SiC wafers

and the requirement of graphitization tools, we envision that monolayer graphene formed on other rigid substrates could also be alternatively used for dry transfer, such as graphene grown on Ge (110) substrates[26] or on copper-deposited substrates.[27] Also, although wet transfer is more commonly used to transfer CVD-grown graphene on copper foils, which is one of the most widely used graphene templates, it is also possible to dry-transfer the graphene on copper foils using polymer stamps[28] or water-assisted oxidation,[29] and thus these approaches could be explored to prepare dry-transferred graphene on III-V substrates for remote epitaxy.

In order to investigate if the principles discovered above are generally applicable for other material systems, we have performed and compared remote epitaxy of other materials with varied interface properties using wet and dry transfer methods. Compared with GaAs which has covalent-ionic mixed bonding characteristics with weak ionicity of 31%,[30] III-N and complex oxides materials exhibit higher ionicity.[31-33] Since substrate materials with higher ionicity provide greater variations in electrostatic potential above graphene, the cohesive ordering of adatoms on graphene for remote epitaxy is facilitated on these high-ionicity materials.[7] We have performed wet- and dry-transfer of graphene onto GaN after deoxidizing GaN surface. Then GaN is grown on graphene *via* molecular beam epitaxy (MBE) with the nominal thickness of 1 μm, and the results are completely different from the case for GaAs. As shown in the EBSD maps in Figure 2e and 2f, both remote epitaxial GaN on wet- and dry-transferred graphene show single-crystallinity. The inverse pole figure maps of in-plane orientation (IPF-X) in Supporting Figure S5 reveal that there is no in-plane rotation, which also confirms the single-crystallinity. This suggests that stronger electrostatic potential fluctuation of GaN than GaAs allows remote interaction even through the wet-transferred graphene at the interface. It should be noted that, however, the remote epitaxial single-crystalline GaN grown on wet-transferred graphene shows surface morphology where the

nucleated films are not fully merged while GaN grown on dry-transferred graphene shows fully merged smooth morphology (Figure 2a and 2b). This finding suggests that interface contamination during wet transfer still affects remote epitaxial growth at the nucleation stage for III-N growths. We further investigated the impact of graphene transfer methods for remote epitaxy of complex oxides. It can be postulated that oxide materials are formed mainly by ionic bonding characters, thus the electrostatic potential from the substrate is strongest while further oxidation cannot occur during wet transfer process such that graphene transfer methods may not affect their remote epitaxial capability. To verify this, we have performed remote epitaxy of $BaTiO_3$ (BTO) on STO substrates coated with graphene *via* wet and dry transfer process. As shown in Figure 2(c,d,g,h), the surface morphology and crystallinity of BTO grown by MBE on wet- and dry-transferred graphene are comparable as postulated and both remote epitaxial BTO films show perfect single-crystallinity. The differences in the remote epitaxial characteristics of GaAs, GaN, and BTO thin films grown on wet- and dry-transferred graphene clearly show the role of the ionicity of materials that governs the intensity of electrostatic potential fluctuations as well as the interface cleanness in remote epitaxy.

For reliable remote interaction of adatoms with the substrate through graphene, it is critically important to preserve the graphene in the harsh epitaxy environment, which is another key challenge. Although graphene is thermally robust under vacuum, it is well known that graphene can be damaged at elevated temperatures by interaction with gaseous molecules or plasma. As an example, treating the graphene surface with N_2 plasma, O_2 plasma, or NH_3 is known to damage the graphene and induce the formation of dangling bonds in graphene.[34-36] Due to the huge alteration of surface free energy around dangling bonds, these dangling bonds can become nucleation sites. Therefore, the growth on damaged graphene could result in quasi-van der Waals

(qvdW) epitaxy, wherein the nucleation is governed by the surface potential of graphene,[37-39] which deviates from remote epitaxial growth mode because the crystal information of the substrate is screened by damaged graphene. More severe damage under the epitaxy environment is partial etching of graphene, and if etching occurs, direct epitaxy from exposed substrate will take place. This will prevent the epitaxial film from exfoliation at the graphene interface and induce substrate spalling. Therefore, it is essential to preserve the graphene from being damaged under the epitaxy environment for remote epitaxy.

In MOCVD growths of III-V materials, hydrogen and nitrogen are two widely used carrier gases to introduce precursors and hydrides into the reactor. The remote epitaxy of single-crystalline GaAs on dry-transferred graphene demonstrated in Figure 1f has employed nitrogen carrier. On the other hand, when hydrogen carrier is employed, GaAs grown on dry-transferred graphene exhibits rough surface morphology, as shown in the scanning electron microscopy (SEM) image in Figure 3a, even though all other sample preparation and growth conditions are identical. The grown film is still well exfoliated at the graphene interface (Figure 3b), suggesting that graphene is not etched away. However, EBSD maps reveal that the GaAs film grown using hydrogen carrier is polycrystalline as shown in Figure 3c. This may be associated with the transition of seeding remotely from the substrate to graphene (remote epitaxy to qvdW epitaxy) and it can be expected that significant difference in lattice of graphene compared to GaAs would not host single-crystalline epitaxy of GaAs. To verify this speculation and understand the effect of the carrier gas on graphene properties, the growth condition is mimicked by annealing the graphene-coated GaAs substrates in low-pressure hydrogen and nitrogen ambient at the GaAs growth temperature of 650 ˚C (See Methods for details). In the case of hydrogen environment, XPS measurements of carbon-related peaks in Figure 3d show significantly increased sp^3 bonding-

related peaks and carbide-related peaks,[22,40] compared with nitrogen-annealed graphene in Figure 3e. In other words, the sp^2-bonded graphene lattice is damaged by hydrogen, forming dangling bonds and metallic carbides (Ga-C and/or As-C), and these results agree with previous reports that hydrogen can break C-C bonds of graphene.[41,42] The same treatment conducted on graphene transferred onto SiO_2/Si shows similar trend, in that significantly broadened XPS spectra are observed only when the graphene is annealed under hydrogen ambient (Supporting Figure S6). Raman spectra in Figure 3f also support such transformation of graphene by hydrogen, in that strong D peak has emerged while 2D peak almost disappeared under hydrogen, revealing the formation of sp^3 bondings. On the other hand, D peak is not observed and the large *I(2D)/I(G)* ratio is maintained after nitrogen annealing (Figure 3g), suggesting that the change of graphene properties is not significant under nitrogen. Therefore, this set of experiments demonstrates that the surface potential fluctuation induced by dangling bonds in damaged graphene can screen the potential fluctuation of the substrate, leading to the nucleation of polycrystalline GaAs, and thus shows that preserving the graphene quality under the epitaxy environment is critically important in remote epitaxy of GaAs. We believe that *in situ* characterizations of the surface of graphene-coated substrates under the harsh epitaxy environment, such as *in situ* XPS or *in situ* transmission electron microscopy (TEM), will shed more light on the changes of the graphene and the interface properties as well as their impact on remote epitaxy. For the more ionic GaN, which provides stronger fluctuations in the electrostatic potential above graphene, remote epitaxy by MOCVD using hydrogen carrier was also reported by other group,[12] implying that the requirement for preserving the graphene quality is less stringent if the penetration of the electrostatic potential through graphene is stronger. Therefore, in summary, both the graphene transfer method and

epitaxy condition need to be carefully controlled for reliable remote epitaxy especially if the ionicity of the material of interest is weak, such as GaAs.

Lastly, we further investigate the possibility of direct epitaxy through defects in graphene which could impact on the crystallinity of epitaxial overlayers on graphene. It is well known that defects such as pinholes and tears can be easily incorporated into graphene during graphene growth, transfer, and remote epitaxy. For macroscopic tearing, the region of tearing can be easily identified by optical microscope imaging, and can also be identified from exfoliation of grown films because spalling of the substrate can be observed from the area where there is no graphene.[6] Nevertheless, such damaged region generally occupies very small portion of the graphene-coated substrate, and does not complicate the study on remote epitaxy. On the other hand, nanoscale defects on graphene, which might be formed by imperfect graphene growth, graphene transfer process, or harsh epitaxy environment, will be hard to identify but could contribute to growth by nucleation on such pinholes followed by lateral overgrowth. To verify the possibility of the nanoscopic damages or pinholes on graphene that can induce mixed growth mode of remote epitaxy and pinhole-based lateral overgrowth, we have employed an elemental material without ionicity as either the substrate or the epitaxial material. This can unambiguously identify whether such effects exist or need to be considered, because elemental materials do not give rise to an electrostatic potential that can permeate the graphene due to non-existence of ionicity in their bonding.[7] Thus, only if lateral overgrowth from those pinholes is a dominant growth mechanism, single-crystalline films can be formed on graphene when elemental materials are involved. We have investigated six possible combinations for remote epitaxy with lattice matching condition, *i.e*. GaAs on Ge, Ge on GaAs, and Ge on Ge, with and without dry-transferred graphene monolayer. All growths are conducted by MOCVD at 650 ˚C using a nitrogen carrier gas (See Methods for detailed growth conditions).

The growth temperature of 650 ˚C is high enough to ensure the pyrolysis of precursors without the need of catalytic effects on GaAs surface, and thus precursors can be effectively decomposed into adatoms and adducts on the surface of graphene despite its inertness, not only on the surface of GaAs and Ge.[43] Here, the EBSD maps of films grown on graphene are measured at the interface side after exfoliation, while those of the films directly grown on the substrate without graphene are measured from the top surfaces, since samples without graphene cannot be exfoliated. As shown in Figure 4(a,c,e), single-crystalline films are successfully grown for all three cases without having graphene on the substrate (Ge-Ge, Ge-GaAs, and GaAs-Ge). On the other hand, randomly oriented polycrystalline films appear on graphene-coated substrates for all three cases as shown in Figure 4(b,d,f) and Supporting Figure S7 (Ge/graphene/Ge, Ge/graphene/GaAs, GaAs/graphene/Ge). The size of Ge grains in Figure 4(b,d) is smaller than that of GaAs grains in Figure 4f, indicating that the diffusion length of Ge adatoms on graphene-coated substrates is shorter than that of Ga or As adatoms. It should be noted that the strength of remote interaction between the substrate and the nucleus at the nucleation stage of remote epitaxy is not solely governed by the polarity of the substrate, but by the polarity of both the substrate and the epitaxial material.[7] Therefore, in heteroepitaxial systems, such as Ge/graphene/GaAs and GaAs/graphene/Ge, the potential energy fluctuation by the displacement of nuclei is larger than Ge/graphene/Ge system, but smaller than GaAs/graphene/GaAs, and the experimental results suggest that the remote interaction in Ge/graphene/GaAs material systems is not strong enough to facilitate lattice alignment between the nuclei and the substrate. The formation of polycrystalline films on graphene clearly indicates that pinhole-based lateral overgrowth through graphene can be excluded as a mechanism for obtaining single-crystalline epitaxy on graphene, and shows that the polarity of both the substrate and the epilayer is the driving force for guided nucleation through

graphene. Moreover, successful epitaxy of single-crystalline films through multilayer graphene layers for materials with high ionicity[7,12,13] also proves that it is the electrostatic potential from the remote substrate that predominantly guides orientation of epitaxial films as microscopic pinholes in a single graphene layer would be sealed by a stack of graphene layers.

Conclusion

In conclusion, we have demonstrated how the properties of graphene, substrate materials, graphene-substrate interface and epitaxial materials affect electrostatic interaction between the adatoms and the substrate through graphene, where the strength of the interaction governs cohesive ordering of adatoms on graphene in remote epitaxy. We have conducted systematic studies on remote epitaxy with various experimental conditions, which has led to the finding of generally applicable principles and key considerations by revealing the impact of respective properties. We have shown that even if the quality of graphene is originally pristine, either the graphene quality or the interface cleanness between the graphene and the substrate can be degraded during the graphene transfer process or under the epitaxy environment. It is therefore necessary to carefully control the entire processes, including graphene preparation, transfer, and epitaxy, for reliable growth of high-quality remote epitaxial films, and such requirement is more stringent for materials with weaker ionic properties, such as III-V, compared with III-N or complex oxides. Lastly, we have identified that the growth mode on dry-transferred graphene is truly and solely remote epitaxial, by comparing the growth with germanium which does not exhibit ionicity. These results exemplify the critical aspects for experimental demonstration of remote epitaxy that can facilitate heterointegration of freestanding membranes in diverse fields and applications.

Methods

Graphene formation and transfer. We used CVD-grown graphene on copper foils for wet transfer processes, and epitaxial graphene on SiC for dry transfer processes. For CVD growth of graphene, copper foil is first cleaned at 1000 ˚C for 30 min under hydrogen, followed by graphene growth under 4 sccm of CH_4 and 70 sccm of H_2 flow for 30 min at 1.9 Torr. The CVD-graphene on copper is transferred onto foreign substrates for remote epitaxy by standard wet transfer process. First, PMMA is spin-coated on the copper foil, and then the graphene formed on the other side of foil is removed by oxygen plasma. Next, the foil is etched in $FeCl_3$ solution, followed by rinsing the PMMA-graphene stack by scooping the stack and transferring onto clean deionized (DI) water several times. The PMMA-graphene stack is scooped in water by substrates for remote epitaxy, such as GaAs, GaN, STO, and Ge. The GaAs, GaN, and Ge substrates were deoxidized by immersing in diluted HCl and cleaning with water right before the scooping process. For the STO substrate, surface preparation was carried out by immersing the STO substrate in buffered oxide etch (BOE) solution for 30 seconds, followed by rinsing in DI water and annealing in a furnace at 1100° C for 5 hours under oxygen overpressure. Atomic force microscopy (AFM) measurement was carried out to ensure TiO_2 terminated step-and-terrace surface of the STO substrate. The substrates with PMMA-graphene stacks are then dried at 65 ˚C and PMMA is removed in acetone. Lastly, the substrate is rinsed with isopropanol and water, and annealed at 120 ˚C for improved adhesion.

Epitaxial graphene is grown on Si-face 4H and 6H-SiC (0001) wafer by sublimation of silicon, with similar results. SiC wafer is first annealed in 10% H_2/Ar ambient at 1500 ˚C for 30 min to remove subsurface damages due to chemical and physical polishing. Then hydrogen is purged from the system and SiC wafer is heated up to 1800 ˚C in argon for 10 min at 700 Torr to

prepare the graphene layer. The graphene layer is exfoliated from the substrate by depositing nickel handling layer and then attaching a thermally releasable tape to peel the graphene-nickel stack. The tape/nickel/graphene stack is attached onto the growth substrates, where the substrates were deoxidized right before attaching, following the same oxide etching procedure as the wet transfer processes. The tape is then released by annealing on a hot plate, and nickel is removed by immersing the sample into nickel etchant, followed by water rinsing and drying. The wet- and dry-transferred graphene cover the center region of the growth substrates, and thus the surface of the substrate materials is exposed at the edge where graphene is not covering.

Remote epitaxy on graphene-coated substrates and exfoliation. GaAs and Ge epitaxy are conducted in a close coupled showerhead MOCVD reactor, using arsine, trimethylgallium and germane as sources of arsenic, gallium and germanium, respectively. The reactor pressure was kept at 100 Torr throughout the growths, using either nitrogen or hydrogen as a carrier gas. GaAs growths were conducted at 650 ˚C with a growth rate of ~33 nm/min on GaAs or Ge substrates with and without graphene. Ge growths were conducted at 650 ˚C with a growth rate of ~30 nm/min using a nitrogen carrier gas on GaAs or Ge substrates with and without graphene.

GaN is grown by MBE, using an effusion gallium cell and plasma-assisted nitrogen as sources of gallium and nitrogen. The growth was conducted at a substrate temperature of 700 ˚C and a RF plasma power of 250W. The growth was initiated under a nitrogen-rich condition for a short period to encourage the nucleation of GaN islands on graphene and then the gallium flux is increased to grow GaN thin film under a gallium-rich condition.

BTO films are grown on graphene covered STO substrates using a Veeco GEN10 MBE system. Conventional effusion cells were used to generate molecular beams of barium and titanium.

RHEED intensity oscillations were used to calibrate the flux, and Ba and Ti were co-deposited in an oxygen partial pressure of 7×10^{-7} torr at a substrate temperature of 850 ˚C.

The remote epitaxial GaAs, GaN, and BTO films are exfoliated by first depositing titanium adhesion layer and nickel stressor layer. Next, a thermally releasable tape is attached on top, and the stack of tape/metal/epitaxial layer is peeled off from the substrate at the graphene interface.

Characterizations. Raman spectra of wet- and dry-transferred graphene were measured using Raman microscopic system (α 300M+, WITec) with a pump laser wavelength of 532 nm. XPS spectra of graphene-coated substrates were measured with a magnesium K-alpha source (MultiLab 2000, Thermo VG) after calibrating the peak with C1s at 285 eV. All XPS data are measured at room temperature, and the energy resolution of the XPS equipment is 0.5 eV. XPS spectra are fitted by Shirley background type and Gaussian-Lorentzian shape lines. The 650 ˚C annealing of graphene-coated GaAs samples for XPS characterization was conducted in a furnace tube at 300 mTorr for 1 hour with nitrogen or hydrogen flow of 100 sccm. AFM measurements were conducted using an AFM probe with a silicon tip (PPP-NCHR, Nanosensors^{TM}) by a non-contact mode (Park NX10, Park Systems).

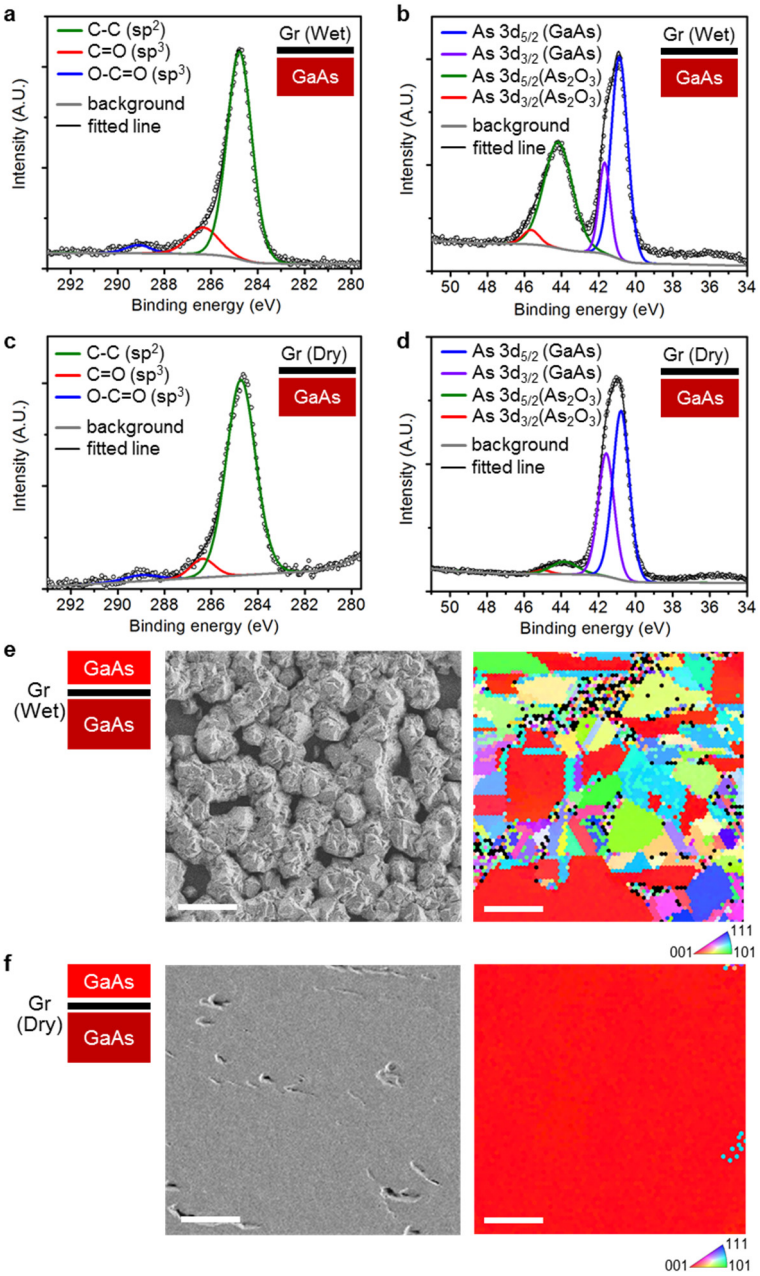

Figure 1. Graphene transfer onto GaAs and remote epitaxy of GaAs. (a) Carbon-related and (b) arsenic-related XPS spectra of graphene/GaAs prepared by wet transfer process, and (c,d) by dry transfer process. (e) Top-view SEM images (left) and EBSD maps (right) of GaAs grown on wet-transferred graphene and (f) on dry-transferred graphene. Scale bars in SEM images, 10 μm. Scale bars in EBSD maps, 2 μm.

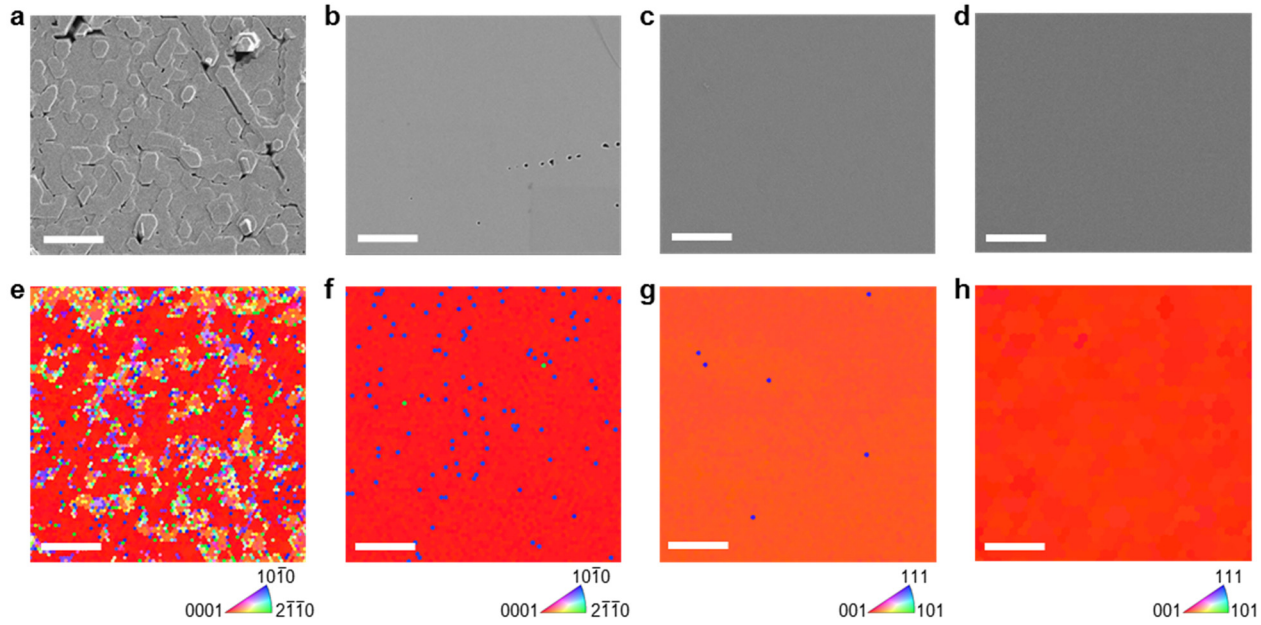

Figure 2. Remote epitaxy of GaN and complex oxides. Top-view SEM images (upper) and EBSD maps (lower) for (a,e) GaN grown on wet transferred Gr/GaN, (b,f) GaN on dry transferred Gr/GaN, (c,g) BTO on wet transferred Gr/STO, and (d,h) BTO on dry transferred Gr/STO. All scale bars, 2 μm.

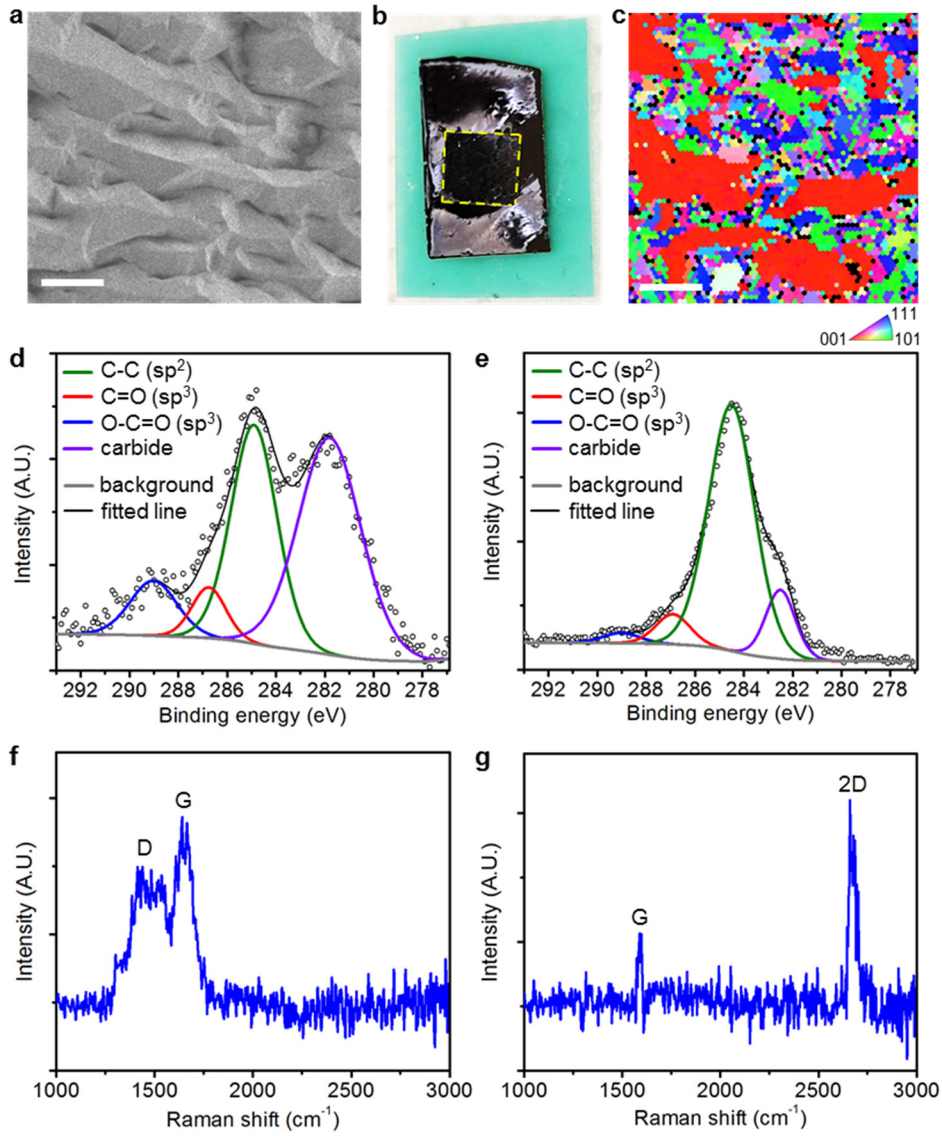

Figure 3. Effect of epitaxy condition on remote epitaxy. (a) Top-view SEM of GaAs grown on dry transferred graphene/GaAs using hydrogen carrier. Scale bar, 10 μm. (b) Photograph of exfoliated GaAs film. The dashed box represents graphene-covered region, which is successfully exfoliated at the graphene interface, while outside of the graphene-covered region is spalled. (c) EBSD map of exfoliated GaAs film. Scale bar, 2 μm. (d) XPS spectra and (f) Raman spectra of hydrogen-treated graphene/GaAs. (e) XPS spectra and (g) Raman spectra of nitrogen-treated graphene/GaAs.

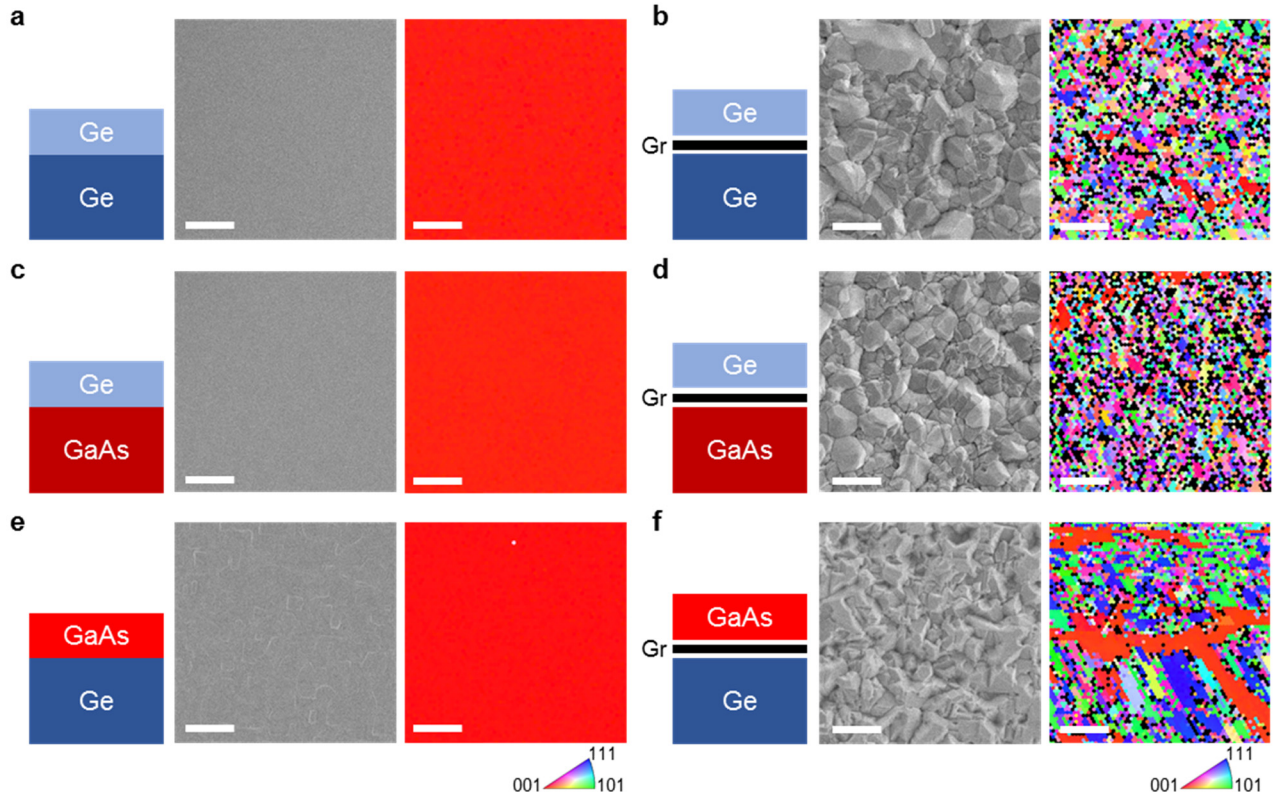

Figure 4. Epitaxy involving elemental materials. Top-view SEM images (left) and EBSD maps (right) of (a) Ge grown on Ge, (b) Ge on graphene/Ge, (c) Ge on GaAs, (d) Ge on graphene/GaAs, (e) GaAs on Ge, and (f) GaAs on graphene/Ge. All scale bars, 2 μm.

ASSOCIATED CONTENT

Supporting Information.

The Supporting Information is available free of charge.

Raman spectra of graphene-coated substrates, AFM image of graphene-coated substrates, XPS spectra of graphene-coated substrates, EBSD map of remote epitaxial films.

AUTHOR INFORMATION

Corresponding Author

*Jeehwan Kim. E-mail: jeehwan@mit.edu.

Author Contributions

H.K. and J.K. conceived the experiment. H.S., J.-H.L. and J.-H.A. prepared CVD graphene. C.D. and J.A.R. prepared epitaxial graphene. H.K., Y.L., H.S.K., K.L., K.Q., S.-H.B., S.L. and C.C. performed graphene transfer and characterization. H.K. and K.L. performed MOCVD growth. Y.L. and K.Q. performed GaN epitaxy. H.S.K., H.P., S.X., J.H.L. and D.G.S. performed BTO epitaxy. H.K., Y.L., H.S.K., K.L., and K.Q. performed exfoliation of grown films and EBSD measurements. K.S.K., Y.J.J., K.H.K., and G.Y.Y. performed XPS and Raman spectra measurements. The manuscript was written through contributions of all authors. All authors have given approval to the final version of the manuscript. †H.K. and K.L. contributed equally.

Notes

The authors declare no competing financial interest.

ACKNOWLEDGMENT

This work is primarily supported by the Defense Advanced Research Projects Agency Young Faculty Award (award no. 029584-00001) and by the U.S. Department of Energy's Office of Energy Efficiency and Renewable Energy (EERE) under the Solar Energy Technologies Office (award no. DE-EE0008558). The team at MIT also acknowledges support from the Air Force Research Laboratory (FA9453-18-2-0017 and FA9453-21-C-0717). C.D. and J.A.R acknowledge the Penn State 2D Crystal Consortium (2DCC)-Materials Innovation Platform (2DCC-MIP) under NSF cooperative agreement DMR- 1539916. The work at Cornell University is supported by the National Science Foundation (Platform for the Accelerated Realization, Analysis and Discovery of Interface Materials (PARADIM)) under Cooperative Agreement Number DMR-1539918.

REFERENCES

1. Kum, H.; Lee, D.; Kong, W.; Kim, H.; Park, Y.; Kim, Y.; Baek, Y.; Bae, S.-H.; Lee, K.; Kim, J., Epitaxial Growth and Layer-Transfer Techniques for Heterogeneous Integration of Materials for Electronic and Photonic Devices. *Nature Electronics* **2019,** *2* (10), 439-450.
2. Yablonovitch, E.; Gmitter, T.; Harbison, J.; Bhat, R., Extreme Selectivity in the Lift-Off of Epitaxial GaAs Films. *Applied Physics Letters* **1987,** *51* (26), 2222-2224.
3. Wong, W.; Sands, T.; Cheung, N., Damage-free Separation of GaN Thin Films from Sapphire Substrates. *Applied Physics Letters* **1998,** *72* (5), 599-601.
4. Bedell, S. W.; Fogel, K.; Lauro, P.; Shahrjerdi, D.; Ott, J. A.; Sadana, D., Layer Transfer by Controlled Spalling. *Journal of Physics D: Applied Physics* **2013,** *46* (15), 152002.
5. Kim, H.-S.; Brueckner, E.; Song, J.; Li, Y.; Kim, S.; Lu, C.; Sulkin, J.; Choquette, K.; Huang, Y.; Nuzzo, R. G., Unusual Strategies for Using Indium Gallium Nitride Grown on Silicon (111) for Solid-State Lighting. *Proceedings of the National Academy of Sciences* **2011,** *108* (25), 10072-10077.
6. Kim, Y.; Cruz, S. S.; Lee, K.; Alawode, B. O.; Choi, C.; Song, Y.; Johnson, J. M.; Heidelberger, C.; Kong, W.; Choi, S., Remote Epitaxy through Graphene Enables Two-Dimensional Material-Based Layer Transfer. *Nature* **2017,** *544* (7650), 340-343.
7. Kong, W.; Li, H.; Qiao, K.; Kim, Y.; Lee, K.; Nie, Y.; Lee, D.; Osadchy, T.; Molnar, R. J.; Gaskill, D. K., Polarity Governs Atomic Interaction through Two-Dimensional Materials. *Nature Materials* **2018,** *17* (11), 999-1004.

8. Guo, Y.; Sun, X.; Jiang, J.; Wang, B.; Chen, X.; Yin, X.; Qi, W.; Gao, L.; Zhang, L.; Lu, Z., A Reconfigurable Remotely Epitaxial VO_2 Electrical Heterostructure. *Nano letters* **2019,** *20* (1), 33-42.
9. Jiang, J.; Sun, X.; Chen, X.; Wang, B.; Chen, Z.; Hu, Y.; Guo, Y.; Zhang, L.; Ma, Y.; Gao, L., Carrier Lifetime Enhancement in Halide Perovskite *via* Remote Epitaxy. *Nature Communications* **2019,** *10* (1), 1-12.
10. Wang, D.; Lu, Y.; Meng, J.; Zhang, X.; Yin, Z.; Gao, M.; Wang, Y.; Cheng, L.; You, J.; Zhang, J., Remote Heteroepitaxy of Atomic Layered Hafnium Disulfide on Sapphire through Hexagonal Boron Nitride. *Nanoscale* **2019,** *11* (19), 9310-9318.
11. Bae, S.-H.; Lu, K.; Han, Y.; Kim, S.; Qiao, K.; Choi, C.; Nie, Y.; Kim, H.; Kum, H. S.; Chen, P., Graphene-Assisted Spontaneous Relaxation towards Dislocation-Free Heteroepitaxy. *Nature Nanotechnology* **2020,** *15* (4), 272-276.
12. Jeong, J.; Wang, Q.; Cha, J.; Jin, D. K.; Shin, D. H.; Kwon, S.; Kang, B. K.; Jang, J. H.; Yang, W. S.; Choi, Y. S., Remote Heteroepitaxy of GaN Microrod Heterostructures for Deformable Light-Emitting Diodes and Wafer Recycle. *Science Advances* **2020,** *6* (23), eaaz5180.
13. Kum, H. S.; Lee, H.; Kim, S.; Lindemann, S.; Kong, W.; Qiao, K.; Chen, P.; Irwin, J.; Lee, J. H.; Xie, S., Heterogeneous Integration of Single-Crystalline Complex-Oxide Membranes. *Nature* **2020,** *578* (7793), 75-81.
14. Jeong, J.; Min, K.-A.; Kang, B. K.; Shin, D. H.; Yoo, J.; Yang, W. S.; Lee, S. W.; Hong, S.; Hong, Y. J., Remote Heteroepitaxy across Graphene: Hydrothermal Growth of Vertical ZnO Microrods on Graphene-Coated GaN Substrate. *Applied Physics Letters* **2018,** *113* (23), 233103.
15. Journot, T.; Okuno, H.; Mollard, N.; Michon, A.; Dagher, R.; Gergaud, P.; Dijon, J.; Kolobov, A.; Hyot, B., Remote Epitaxy Using Graphene Enables Growth of Stress-Free GaN. *Nanotechnology* **2019,** *30* (50), 505603.
16. Kong, W.; Kum, H.; Bae, S.-H.; Shim, J.; Kim, H.; Kong, L.; Meng, Y.; Wang, K.; Kim, C.; Kim, J., Path towards Graphene Commercialization from Lab to Market. *Nature Nanotechnology* **2019,** *14* (10), 927-938.
17. Suk, J. W.; Kitt, A.; Magnuson, C. W.; Hao, Y.; Ahmed, S.; An, J.; Swan, A. K.; Goldberg, B. B.; Ruoff, R. S., Transfer of CVD-Grown Monolayer Graphene onto Arbitrary Substrates. *ACS Nano* **2011,** *5* (9), 6916-6924.
18. Kim, J.; Park, H.; Hannon, J. B.; Bedell, S. W.; Fogel, K.; Sadana, D. K.; Dimitrakopoulos, C., Layer-Resolved Graphene Transfer *via* Engineered Strain Layers. *Science* **2013,** *342* (6160), 833-836.
19. Bae, S.-H.; Zhou, X.; Kim, S.; Lee, Y. S.; Cruz, S. S.; Kim, Y.; Hannon, J. B.; Yang, Y.; Sadana, D. K.; Ross, F. M., Unveiling the Carrier Transport Mechanism in Epitaxial Graphene for Forming Wafer-Scale, Single-Domain Graphene. *Proceedings of the National Academy of Sciences* **2017,** *114* (16), 4082-4086.
20. Ferrari, A. C.; Basko, D. M., Raman Spectroscopy as a Versatile Tool for Studying the Properties of Graphene. *Nature Nanotechnology* **2013,** *8* (4), 235-246.

21. Hao, Y.; Wang, Y.; Wang, L.; Ni, Z.; Wang, Z.; Wang, R.; Koo, C. K.; Shen, Z.; Thong, J. T., Probing Layer Number and Stacking Order of Few-Layer Graphene by Raman Spectroscopy. *Small* **2010,** *6* (2), 195-200.
22. Bomben, K. D.; Moulder, J. F.; Sobol, P. E.; Stickle, W. F., *Handbook of X-Ray Photoelectron Spectroscopy.* Perkin-Elmer Corporation: Eden Prairie, **1992**.
23. Bae, S.; Kim, H.; Lee, Y.; Xu, X.; Park, J.-S.; Zheng, Y.; Balakrishnan, J.; Lei, T.; Kim, H. R.; Song, Y. I., Roll-to-Roll Production of 30-Inch Graphene Films for Transparent Electrodes. *Nature Nanotechnology* **2010,** *5* (8), 574.
24. Bunch, J. S.; Verbridge, S. S.; Alden, J. S.; Van Der Zande, A. M.; Parpia, J. M.; Craighead, H. G.; McEuen, P. L., Impermeable Atomic Membranes from Graphene Sheets. *Nano Letters* **2008,** *8* (8), 2458-2462.
25. Berry, V., Impermeability of Graphene and Its Applications. *Carbon* **2013,** *62*, 1-10.
26. Lee, J.-H.; Lee, E. K.; Joo, W.-J.; Jang, Y.; Kim, B.-S.; Lim, J. Y.; Choi, S.-H.; Ahn, S. J.; Ahn, J. R.; Park, M.-H., Wafer-Scale Growth of Single-Crystal Monolayer Graphene on Reusable Hydrogen-Terminated Germanium. *Science* **2014,** *344* (6181), 286-289.
27. Hu, B.; Ago, H.; Ito, Y.; Kawahara, K.; Tsuji, M.; Magome, E.; Sumitani, K.; Mizuta, N.; Ikeda, K.-I.; Mizuno, S., Epitaxial Growth of Large-Area Single-Layer Graphene over Cu (111)/Sapphire by Atmospheric Pressure CVD. *Carbon* **2012,** *50* (1), 57-65.
28. Lock, E. H.; Baraket, M.; Laskoski, M.; Mulvaney, S. P.; Lee, W. K.; Sheehan, P. E.; Hines, D. R.; Robinson, J. T.; Tosado, J.; Fuhrer, M. S., High-Quality Uniform Dry Transfer of Graphene to Polymers. *Nano Letters* **2012,** *12* (1), 102-107.
29. Luo, D.; You, X.; Li, B.-W.; Chen, X.; Park, H. J.; Jung, M.; Ko, T. Y.; Wong, K.; Yousaf, M.; Chen, X., Role of Graphene in Water-Assisted Oxidation of Copper in Relation to Dry Transfer of Graphene. *Chemistry of Materials* **2017,** *29* (10), 4546-4556.
30. Phillips, J., Ionicity of the Chemical Bond in Crystals. *Reviews of Modern Physics* **1970,** *42* (3), 317.
31. Catlow, C.; Stoneham, A., Ionicity in Solids. *Journal of Physics C: Solid State Physics* **1983,** *16* (22), 4321.
32. Turik, A.; Khasabov, A., Localized and Delocalized Models in the Theory of Polarization: Perovskite Oxides. *Journal of Physics: Condensed Matter* **1998,** *10* (11), 2477.
33. Qteish, A., Electronegativity Scales and Electronegativity-Bond Ionicity Relations: A Comparative Study. *Journal of Physics and Chemistry of Solids* **2019,** *124*, 186-191.
34. Wang, Z.-j.; Wei, M.; Jin, L.; Ning, Y.; Yu, L.; Fu, Q.; Bao, X., Simultaneous N-Intercalation and N-Doping of Epitaxial Graphene on 6H-SiC (0001) through Thermal Reactions with Ammonia. *Nano Research* **2013,** *6* (6), 399-408.
35. Yadav, R.; Dixit, C., Synthesis, Characterization and Prospective Applications of Nitrogen-Doped Graphene: A Short Review. *Journal of Science: Advanced Materials and Devices* **2017,** *2* (2), 141-149.
36. Chung, K.; Lee, C.-H.; Yi, G.-C., Transferable GaN Layers Grown on ZnO-Coated Graphene Layers for Optoelectronic Devices. *Science* **2010,** *330* (6004), 655-657.

37. Kovács, A.; Duchamp, M.; Dunin-Borkowski, R. E.; Yakimova, R.; Neumann, P. L.; Behmenburg, H.; Foltynski, B.; Giesen, C.; Heuken, M.; Pécz, B., Graphoepitaxy of High-Quality GaN Layers on Graphene/6H–SiC. *Advanced Materials Interfaces* **2015,** *2* (2), 1400230.

38. Wu, Q.; Yan, J.; Zhang, L.; Chen, X.; Wei, T.; Li, Y.; Liu, Z.; Wei, X.; Zhang, Y.; Wang, J., Growth Mechanism of AlN on Hexagonal BN/sapphire Substrate by Metal–Organic Chemical Vapor Deposition. *CrystEngComm* **2017,** *19* (39), 5849-5856.

39. Araki, T.; Uchimura, S.; Sakaguchi, J.; Nanishi, Y.; Fujishima, T.; Hsu, A.; Kim, K. K.; Palacios, T.; Pesquera, A.; Centeno, A., Radio-Frequency Plasma-Excited Molecular Beam Epitaxy Growth of GaN on Graphene/Si (100) Substrates. *Applied Physics Express* **2014,** *7* (7), 071001.

40. El Mel, A.-A.; Gautron, E.; Choi, C.; Angleraud, B.; Granier, A.; Tessier, P.-Y., Titanium Carbide/Carbon Composite Nanofibers Prepared by a Plasma Process. *Nanotechnology* **2010,** *21* (43), 435603.

41. Wang, W.; Li, Y.; Zheng, Y.; Li, X.; Huang, L.; Li, G., Lattice Structure and Bandgap Control of 2D GaN Grown on Graphene/Si Heterostructures. *Small* **2019,** *15* (14), 1802995.

42. Al Balushi, Z. Y.; Wang, K.; Ghosh, R. K.; Vilá, R. A.; Eichfeld, S. M.; Caldwell, J. D.; Qin, X.; Lin, Y.-C.; DeSario, P. A.; Stone, G., Two-Dimensional Gallium Nitride Realized *via* Graphene Encapsulation. *Nature Materials* **2016,** *15* (11), 1166-1171.

43. Stringfellow, G. B., *Organometallic Vapor-Phase Epitaxy: Theory and Practice*. Elsevier: Amsterdam, **1999**.

For table of contents only (ToC graphic)